http://www.kidney-international.org

see commentary on page 11

Early chronic kidney disease–mineral bone disorder stimulates vascular calcification

Yifu Fang[1], Charles Ginsberg[1], Toshifumi Sugatani[1], Marie-Claude Monier-Faugere[2], Hartmut Malluche[2] and Keith A. Hruska[1]

[1]*Division of Pediatric Nephrology, Department of Pediatrics, Washington University, St Louis, Missouri, USA and*
[2]*Division of Nephrology, Department of Medicine, University of Kentucky, Lexington, Kentucky, USA*

The chronic kidney disease–mineral and bone disorder (CKD–MBD) syndrome is an extremely important complication of kidney diseases. Here we tested whether CKD–MBD causes vascular calcification in early kidney failure by developing a mouse model of early CKD in a background of atherosclerosis-stimulated arterial calcification. CKD equivalent in glomerular filtration reduction to human CKD stage 2 stimulated early vascular calcification and inhibited the tissue expression of α-klotho (klotho) in the aorta. In addition, osteoblast transition in the aorta was stimulated by early CKD as shown by the expression of the critical transcription factor Runx2. The ligand associated with the klotho-fibroblast growth factor receptor complex, FGF23, was found to be expressed in the vascular media of sham-operated mice. Its expression was decreased in early CKD. Increased circulating levels of the osteocyte-secreted proteins, FGF23, and sclerostin may have been related to increased circulating klotho levels. Finally, we observed low-turnover bone disease with a reduction in bone formation rates more than bone resorption. Thus, the CKD–MBD, characterized by cardiovascular risk factors, vascular calcification, increased circulating klotho, FGF23 and sclerostin levels, and low-turnover renal osteodystrophy, was established in early CKD. Early CKD caused a reduction of vascular klotho, stimulated vascular osteoblastic transition, increased osteocytic secreted proteins, and inhibited skeletal modeling producing the CKD–MBD.

Kidney International (2013) **85,** 142–150; doi:10.1038/ki.2013.271; published online 24 July 2013

KEYWORDS: CKD–MBD; FGF23; α-klotho; vascular calcification

Correspondence: *Keith A. Hruska, Division of Pediatric Nephrology, Department of Pediatrics, Washington University, 660 S Euclid Avenue, Campus Box 8208, St Louis, Missouri 63110, USA.*
E-mail: hruska_k@kids.wustl.edu

Received 24 January 2013; revised 9 May 2013; accepted 16 May 2013; published online 24 July 2013

The chronic kidney disease–mineral and bone disorder (CKD–MBD) syndrome is an extremely important complication of kidney diseases. The CKD–MBD was named in 2006,[1] following the realization that the mineral and skeletal disorders accompanying kidney failure are important contributors to the CKD-associated cardiovascular disease and high mortality rates.[2–5] Recent studies have suggested that the CKD–MBD, defined as biochemical abnormalities in mineral metabolism, abnormalities in skeletal remodeling, and extraskeletal calcification, is present when the glomerular filtration is reduced by more than 40%.[6] Within the concept of the CKD–MBD, recent progress related to cardiovascular disease risk factors stimulated by kidney disease has uncovered three: vascular calcification, phosphorus, and fibroblast growth factor 23 (FGF23).[7–11] Vascular calcification particularly poses an increased risk of cardiovascular and all-cause mortality,[7,12] and of the clinical conditions associated with vascular calcification, the most extensive calcifications occur in CKD.[13] In CKD, vascular calcification is stimulated by hyperphosphatemia and positive calcium balance.[14–18]

Emerging data indicate that the CKD–MBD syndrome may begin early in the course of kidney disease and precede the development of clinically detectable abnormalities in plasma phosphorus (Pi), calcium (Ca), parathyroid hormone (PTH), and calcitriol, which are the hallmarks of the established CKD–MBD. Biomarkers of skeletal osteocyte function have been found to be abnormal early in kidney disease, both clinically and in translational models,[6,19–23] indicating that kidney injury had affected the skeleton, in other words, the CKD–MBD had begun. Pereira *et al.*[19] found by skeletal immunocytochemistry and plasma levels that osteocyte production of FGF23 and dentin matrix protein-1 was increased in stage 2 CKD. These results were confirmed by Sabbagh *et al.*[21] and Oliveira *et al.*,[22] who also found that osteocyte sclerostin was increased in early CKD, and that osteocyte nuclear β-catenin was decreased, indicating decreased osteocyte Wnt activity in early CKD. As Wnt activity is the major skeletal anabolic principle of the postnatal skeleton,[24,25] these results indicate that kidney disease signals a decrease in bone formation. Fang *et al.*[20] showed, in a translational model of early CKD, elevated

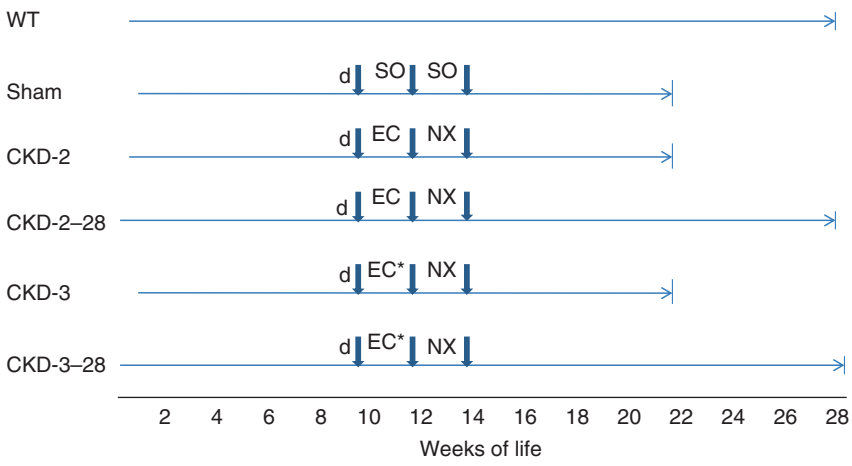

Figure 1 | A schematic drawing of the experimental design defining the various animal groups. WT, wild-type C57B6J mice were used to establish normative parameters; Sham, *low-density lipoprotein–deficient* (*ldlr−/−*) mice on a high-fat diet (d) undergoing sham operations (SO) are the control mice for the effects of chronic kidney disease (CKD); CKD-2, *ldlr−/−* high fat–fed mice undergoing mild renal injury (EC) and contralateral nephrectomy (NX) with killing at 22 weeks; CKD-2–28, same as CKD-2 but killing at 28 weeks (6 additional weeks of slowly progressive CKD); CKD-3, *ldlr−/−* high fat–fed mice undergoing moderate renal injury (EC*) and NX with killing at 22 weeks; CKD-3–28, same as CKD-3 but killing at 28 weeks.

FGF23 levels in the presence of normal plasma Ca, Pi, PTH, and calcitriol, and a decrease in bone formation rates. These results confirmed earlier reports before FGF23 studies from our laboratory that when Ca, Pi, calcitriol, and PTH were maintained normal in CKD, decreased bone formation rates and the adynamic bone disorder were observed.[26] However, it is unknown whether vascular calcification and renal osteodystrophy produced by kidney disease[27,28] are present in the early stages of the CKD–MBD.

These studies were conducted to test the hypothesis that the CKD–MBD begins early in kidney disease, including the onset of heightened cardiovascular risk related to vascular calcification. We developed an animal model of early CKD using the atherosclerosis-bearing low-density lipoprotein–deficient mouse (*ldlr−/−*) fed high-fat, Western-type diets (40% of calories from fat). The phenotype of these mice is further characterized by insulin resistance progressing to type 2 diabetes over time. The mice respond as humans to atherosclerosis with neointimal plaque calcification that is stimulated by advanced CKD.[29] Using inulin clearances to determine glomerular filtration rate (GFR), we staged CKD in mice and developed a model of CKD equivalent in GFR to stage 2 human CKD using unilateral renal injury and contralateral nephrectomy. This model mimics acute kidney injury (AKI) and incomplete recovery in humans with atherosclerosis and insulin resistance/diabetes. The peak GFR (representing a 25–40% decrease from normal GFR) established after recovery from AKI slowly diminished over weeks related to interstitial inflammation and fibrosis, allowing the development of the CKD–MBD. By using this model, we characterized the early CKD–MBD discovering stimulated vascular calcification in early CKD before hyperphosphatemia. The discovery of vascular calcification early in CKD produced a requisite search for mechanisms, and we discovered mesenchymal transition in vascular cells and newly recognized abnormalities in the arterial tree that cause vascular calcification, reduction of vascular klotho,[30–32] expression of FGF23, and increased circulating klotho (c-klotho). The elevations in c-klotho explain the early stimulation of skeletal osteocytes and FGF23 secretion independent of changes in the serum phosphorus.

RESULTS

Studies in early CKD

The overall experimental design is shown in Figure 1. The serum/plasma chemistries (blood urea nitrogen (BUN), Ca, Pi, and PTH) determined in the experimental groups are shown in Table 1. The BUN of wild-type and sham-operated mice ranged from 20 to 23 mg/dl (Table 1). In mice with mild renal ablation, referred to in this paper as CKD-2, the mean BUN of the group was not elevated at 22 weeks and only increased to 24–30 mg/dl at 28 weeks (CKD-2–28). Inulin clearances confirmed a 33% reduction in GFR in the 22-week *ldlr−/−* CKD-2 group (Figure 2). A 40% reduction from normal GFR is the low end of the GFR range in human stage 2 CKD. The CKD-2 animals were normocalcemic and normophosphatemic at 22 weeks (Table 1). In the 28-week CKD-2–28 animals, compatible with the slight progression of the kidney insufficiency, hyperphosphatemia had developed (12.7 ± 3.9 mg/dl). These findings are compatible with our previous findings of hyperphosphatemia in mice with more severe ablation and GFR in the human stage 3 CKD range.[14,33] PTH levels were elevated to 120 ± 48 pg/ml in the CKD-2 animals at 22 weeks, but were only 90.8 ± 20 pg/ml at 28 weeks (not significantly different from the normal levels of the sham-operated animals). The elevation of PTH at 22 weeks in the CKD-2/3 groups following mild renal injury suggests that the elevation may have been related to changes associated with the AKI phase of the model. As shown in Figure 3a, longitudinal analysis of PTH levels

Table 1 | Serum and plasma chemistries and PTH levels

Experiment groups	BUN (mg/dl)	Ca (mg/dl)	Pi (mg/dl)	PTH (pg/ml)
WT, wild-type C57BL6	22.4 ± 4.6	8.28 ± 1.8	8.85 ± 0.2	70.2 ± 10.9
Sham, *ldlr* −/− high fat	20.6 ± 3.7	8.96 ± 0.8	7.92 ± 2.3	74.5 ± 35.4
CKD-2, *ldlr* −/− high fat (22 weeks)	21.1 ± 2.8	7.94 ± 1.2	8.8 ± 3.5	120 ± 48
CKD-2–28 *ldlr* −/− high fat (28 weeks)	27.5 ± 4*#	8.8 ± 1.4	12.7 ± 3.9*#	90.8 ± 20
CKD-3 *ldlr* −/− high fat (22 weeks)	43.7 ± 7.5*#	10.8 ± 0.7*#	11.78 ± 1.9*#	NA
CKD-3–28 *ldlr* −/− high fat (28 weeks)	53.3 ± 13.4*#	11.13 ± 1.5*#	13 ± 2.7*#	467 ± 125*#

Abbreviations: BUN, blood urea nitrogen; Ca, calcium; CKD, chronic kidney disease; ldlr −/− low-density lipoprotein-deficient; NA, not available; Pi, phosphorus; PTH, parathyroid hormone; WT, wild type.
*$P < 0.01$ compared with sham.
#$P < 0.01$ compared with CKD-2.
Number of animals per group '$N = 8$–21.'

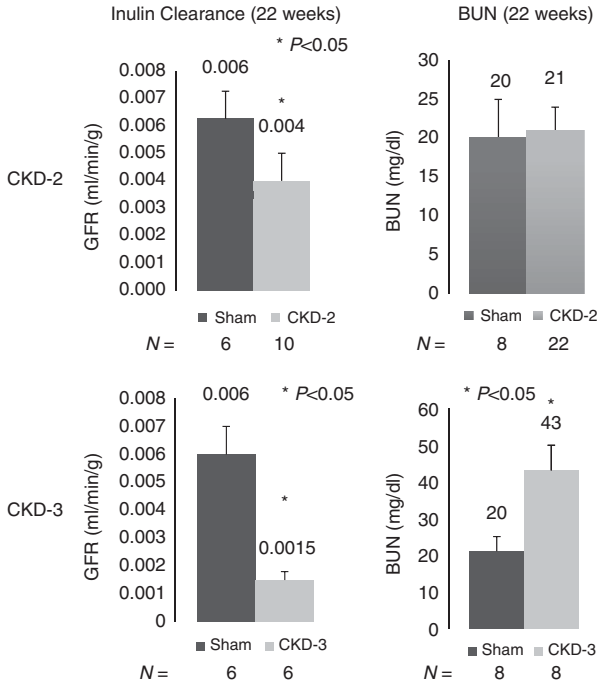

Figure 2 | Inulin clearances in *low-density lipoprotein–deficient* (*ldlr* −/−) high fat–fed mice. Sham-operated mice had inulin clearances of 0.006 ml/min/g. The mild renal injury group (chronic kidney disease (CKD)-2) had reductions in inulin clearance (glomerular filtration rate (GFR)) up to 40% (mean 33%) of the sham-operated control levels. The blood urea nitrogen (BUN) levels were not different between sham-operated and CKD-2 mice. More severe renal injury (CKD-3) produced inulin clearance reductions of 75% in CKD-3 mice and elevations in BUN levels to the 45 mg/dl range. Inulin clearances and BUN levels were determined at 22 weeks of age.

demonstrated threefold elevations of PTH during the AKI phase (15 weeks, 1 week after surgery) that progressively diminished to levels insignificantly elevated from normal at 28 weeks.

Plasma FGF23 levels measured by the Kainos intact hormone assay were elevated by CKD-2 (Figure 3b). FGF23 levels progressively increased from 15 to 22 weeks in the face of normophosphatemia, and continued to rise with the development of hyperphosphatemia in CKD-2–28 instead of diminishing, similar to PTH levels, which was compatible with FGF23 being the basis for the decrease in PTH levels.[34] The use of a domestic FGF23 assay detecting the C-terminus of FGF23 (Immunotopics, Stillwater, MN) demonstrated elevated levels similar to the intact hormone assay at 28 weeks in the CKD-2–28 group (Figure 3c and d). These results suggest the role of FGF23 in maintaining phosphate homeostasis in early CKD.

Aortic and large artery calcification is a critical component of the CKD–MBD, producing vascular stiffness and increased cardiovascular disease in CKD.[35] Vascular calcification in the CKD-2 mice was studied by histology and determination of the aortic Ca content in mg/g dry weight. The CKD-2–28 mice had aortic medial narrowing and advential hyperplasia, but there was no clear evidence of Ca deposition in the media by Alizarin red (Figure 4) or the less sensitive von Kossa (not shown) staining. Aortic Ca content was significantly increased in the CKD-2–28 mice compared with the sham-operated control mice (Figure 4b), and we observed detectable increases in the neointimal atherosclerotic plaque Ca deposits as shown below for the CKD-3–28 mice similar to that previously reported in stage 4 CKD.[29]

Osteoblastic transition of neointimal cells in atherosclerotic lesions has been shown to be critical in the pathogenesis of vascular calcification stimulated by CKD-3–28 in the *ldlr* −/− high fat–fed mouse model,[36] and other studies using different models have shown that osteoblastic transition is involved in medial calcification.[13,37,38] Therefore, we examined whether cells in the aortas of our mice with early CKD expressed evidence of osteoblastic transition. The critical osteoblast transcription factor Runx2 has been shown to be expressed in calcifying vessels, and it serves as the hallmark of osteoblastic transition of cells in the vasculature. We found Runx2 to be strongly expressed in the aortas of our CKD-2–28 mice (Figure 5a). Furthermore, as osteocytes differentiate from osteoblasts, and osteocytes are the main source of FGF23, we examined aortas for FGF23 expression. As shown in Figure 5b, there was significant expression of FGF23 in the aortas of our sham-operated *ldlr* −/− high fat–fed mice, which was reduced by CKD-2 induction. Immunohistochemical analysis of aortic FGF23 expression (Figure 5c) revealed occasional cells in the aortic media of sham-operated mice positive for FGF23. This was lost in the media of CKD-2 mice, replaced by increased advential staining of unknown nature. An advential reaction

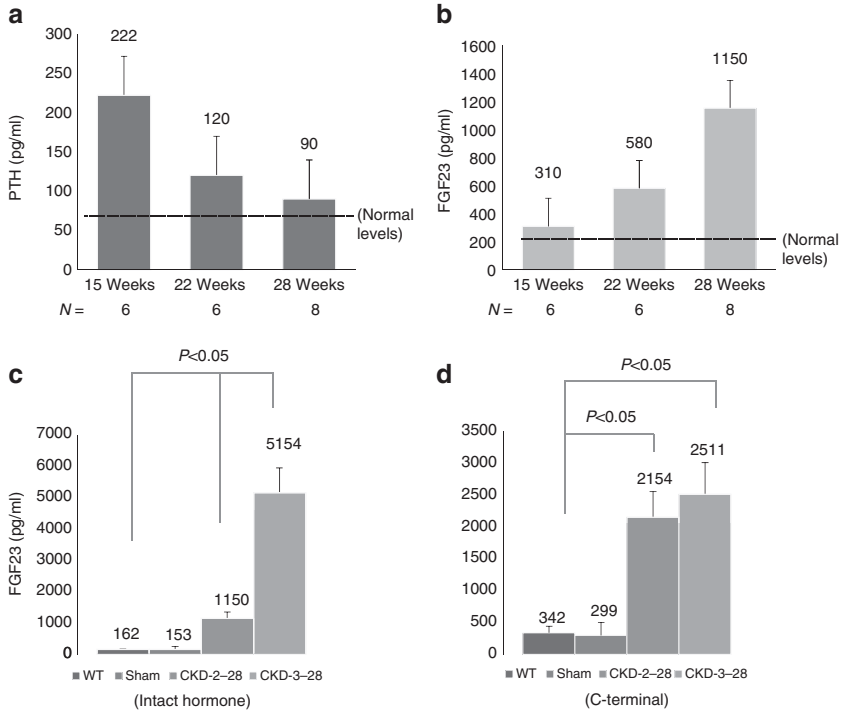

Figure 3 | Longitudinal analysis of parathyroid hormone (PTH) and fibroblast growth factor 23 (FGF23) levels in *low-density lipoprotein–deficient* (*ldlr* − / −) high fat–fed mice with chronic kidney disease (CKD)-2 and CKD-2–28, and FGF23 levels in *ldlr* − / − high fat–fed mice with CKD-2–28 and CKD-3–28. (**a**, **b**) CKD was established at 14 weeks of age as described in methods and Figure 1. Plasma was obtained at 15, 22, and 28 weeks. FGF23 was measured using an intact hormone assay (Kainos). (**c**, **d**) Two different enzyme-linked immunosorbent assays (ELISAs) for FGF23, an intact hormone assay and a C-terminal assay, as described in Materials and Methods, were used to determine the effects of CKD on FGF23 levels in the circulation. FGF23 levels in C57Bl6J wild-type (WT) mice were measured to establish the reference range. FGF23 levels measured using the intact hormone assay were increased in CKD-3–28 mice compared with CKD-2–28, but not when the C-terminal assay was used.

was also detected when a nonspecific IgG (Total IgG) was used in place of the primary antibody (Figure 5c), but it was clearly distinct from the strong reactivity induced by CKD. As the advential reaction exactly matched the immunolocalization of FGFR1 (not shown), one possibility is that this reaction represented FGF23 from the circulation bound to its receptor. The expression of the FGF23/klotho hormonal axis in the aorta was further examined by analysis of klotho expression in the aorta. As shown in Figure 5a, there was significant expression of klotho in the sham-operated control mice, and induction of CKD-2 markedly decreased klotho expression. These results are in agreement with the recent findings of klotho expression in human vascular media by Lim *et al.*[32] As shown in Figure 5c, compared with FGF23, which was expressed in occasional cells and decreased by CKD stage 2, α-klotho was strongly expressed in the media of aortas of wild-type and sham-operated *ldlr* − / − high fat–fed mice, and severely depressed in the media of mice with CKD stage 2. In contrast to the reduction in α-klotho in the vasculature, the circulating hormonal form of klotho, cut klotho or c-klotho, which derives from proteolytic cleavage of renal distal tubular α-klotho,[39] was elevated several fold in the CKD-2 mice (Figure 5d).

The skeletons of the CKD-2–28 mice were analyzed by micro-computed tomography scanning and histomorphometry of trabecular bone. Significant trabecular osteodystrophy was discovered in the *ldlr* − / − high fat–fed sham-operated mice that produced a decrease in trabecular bone volume and trabecular number and thickness (Supplementary Figure S1 online). The osteodystrophy was affected by CKD-2–28 through a decrease in total area. Histomorphometric analysis confirmed the osteodystrophy of the sham-operated *ldlr* − / − high fat–fed mice, and demonstrated the effects of CKD-2–28. Bone formation rates/bone surface were $2.29 \pm 1.49\ mm^3/cm^2$ per year in 28-week-old wild-type C57Bl6J mice used as the normal reference. They were $1.64 \pm 0.67\ mm^3/cm^2$ per year in the sham-operated *ldlr* − / − high fat–fed control mice and $0.87\ mm^3/cm^2$ per year in the CKD-2–28 mice ($P < 0.05$ compared with the sham).

A cortical bone osteodystrophy was also observed by micro-computed tomography in the *ldlr* − / − high fat–fed sham-operated mice. The osteodystrophy was worsened by the induction of stage 2 CKD characterized by cortical bone thinning (loss of total volume) and porosity (decrease in BMD; Figure 6).

In mice undergoing more severe renal ablation and reduction of GFR to levels equal to human stage 3 CKD (CKD-3, and CKD-3–28), the BUN levels were increased to between 35 and 55 mg/dl (Table 1), and the animals were

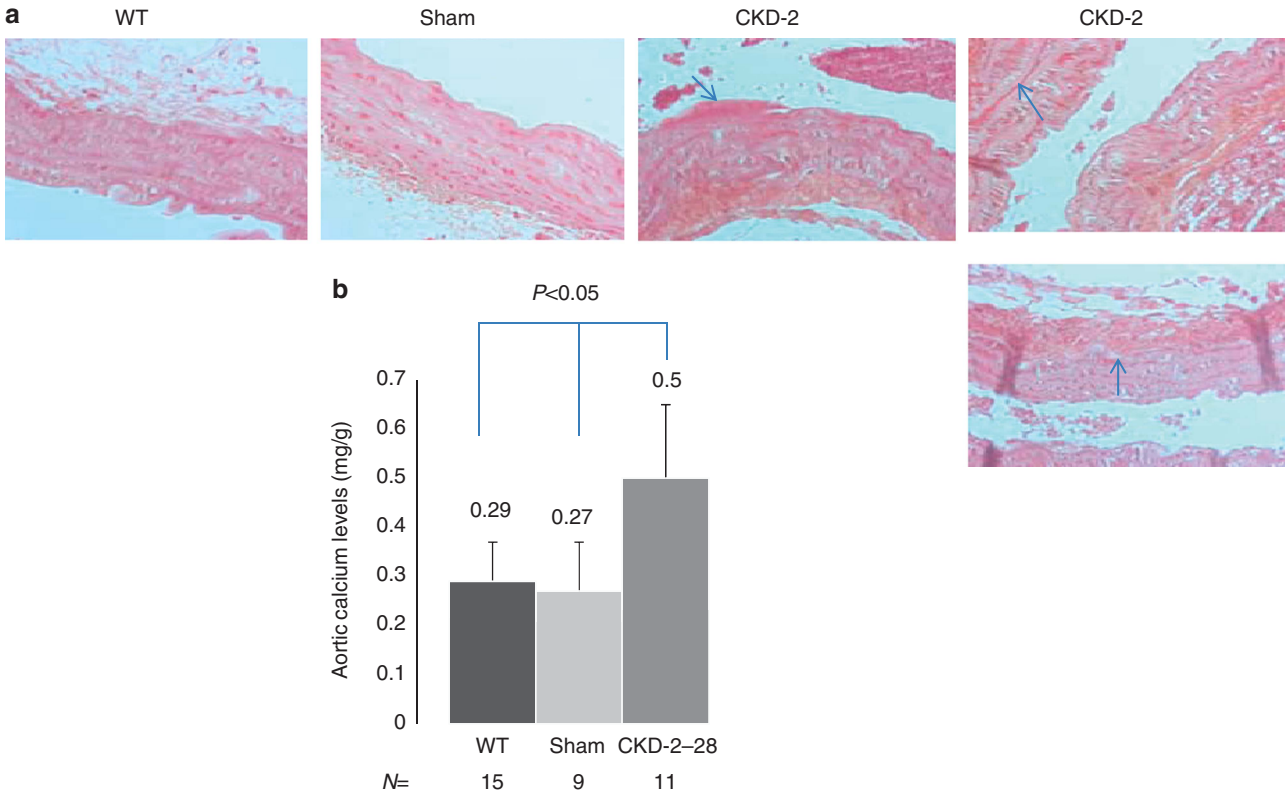

Figure 4 | Aortic calcium (Ca) levels are increased by chronic kidney disease (CKD)-2–28 in *low-density lipoprotein–deficient* (*ldlr −/−*) high fat–fed mice. (**a**) Alizarin red staining revealed questionable early aortic Ca deposition along elastic laminae (arrows) in *ldlr −/−* high fat–fed mice with CKD-2–28 compared with sham-operated mice. WT, wild type. Von Kossa staining of adjacent sections (not shown) was negative. (**b**) CKD-2–28 significantly increased aortic Ca content.

hypercalcemic. PTH levels in the CKD-3–28 mice were very high compared with the near-normal levels observed in CKD-2–28 mice (Table 1). FGF23 levels were significantly more elevated in the CKD-3–28 mice than in the CKD-2–28 mice using the intact hormone assay, whereas the C-terminal assay results were similar to CKD-2–28 values (Figure 3c and d). CKD-3–28 significantly increased the number and size of aortic neointimal plaque calcifications without prominent media calcification detected on Alizarin red (Supplementary Figure S2a online) or von Kossa staining (not shown) of aortic sections. Aortic Ca content of CKD-3–28 mice was significantly increased compared with the sham-operated control mice, and was above the levels found in the aortas of CKD-2–28 mice (Supplementary Figure S2b online).

Finally, we examined the levels of another supposed osteocytic biomarker protein, sclerostin, implicated in CKD and the CKD–MBD to correlate with bone turnover.[40] As shown in Supplementary Figure S3 online, sclerostin levels were significantly increased in the CKD-2–28 mice, more so than in the CKD-3–28 mice.

DISCUSSION

The studies presented here demonstrate that CKD-stimulated vascular calcification begins early in the disease. In our model of early kidney disease in the *ldlr −/−* high fat–fed atherosclerotic mouse, reduction of GFR equivalent to stage 2 human CKD was associated with a significant increase in aortic Ca content, demonstrating vascular calcification. The vascular calcification was early, as histological staining did not reveal clear evidence of medial Ca deposition, and the extensive lesions seen in mice with more severe CKD on high Pi diets were not detected.[15] Our results show the onset of CKD-stimulated vascular calcification before hyperphosphatemia and without high phosphate intake used by El-Abbadi *et al.*[15] In addition, they demonstrate the development of vascular calcification earlier than the greater than 40% reduction in GFR suggested by Moe *et al.*[6] Examination of atherosclerotic plaques failed to demonstrate the extensive Ca deposits stimulated by CKD stage 3/4 that we have previously reported,[14,29,33] although neointimal plaque Ca deposits were increased in the CKD-3 mice, as shown here in Supplementary Figure S2 online. Thus, the vascular calcification stimulated in our model by mild CKD is early and most likely amenable to intervention, because visibly detectable deposits would not have to be reversed.

Key mechanisms of vascular calcification were shown to be present in the aortas of normophosphatemic mice with early CKD (CKD-2). Mesenchymal transition to the osteoblastic lineage in the arterial tree is a well-established mechanism of CKD-stimulated vascular calcification,[13,36,37,41] and vascular

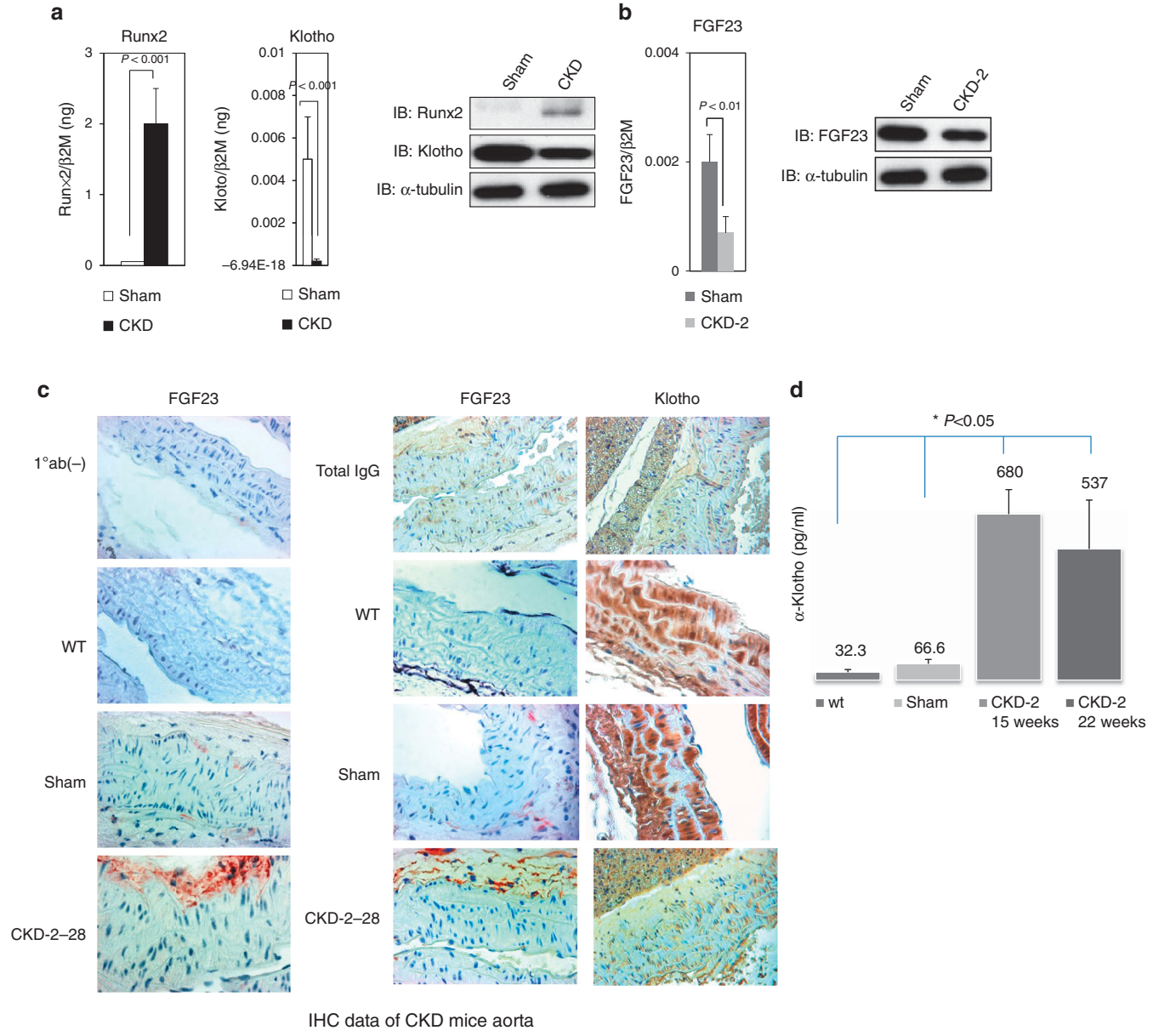

Figure 5 | Osteoblastic transition and detection of fibroblast growth factor 23 (FGF23) and klotho expression in aortas of chronic kidney disease (CKD)-2–28 *low-density lipoprotein-deficient* (*ldlr* − / −) mice. (**a**, **b**) Real-time PCR (RT-PCR) and western blotting (IB) were used to measure (**a**) Runx2, klotho, and (**b**) FGF23 expression in aortas of sham and CKD-2–28 mice. (**c**) Immunolocalization of aortic FGF23 and klotho. (**d**) Plasma levels of circulating klotho (c-klotho). (**a**) CKD-2–28 increased Runx2 expression and decreased α-Klotho expression compared with sham-operated controls as determined by real-time RT-PCR (left) and by western blotting (right); $n = 5$ for RT-PCR. The representative western blots were uniform for five CKD-2–28 mice. (**b**) FGF23 was expressed in the sham-operated control mice and decreased with induction of CKD-2–28; $n = 5$ for RT-PCR. The representative western blots were uniform for five CKD-2–28 mice. (**c**) Antibodies to FGF23 and Klotho, as described in Materials and Methods, were used for the detection of expression in the aortas of the various groups of mice. FGF23 was expressed in occasional cells in the media (two representative sham mice are shown), which was absent in CKD-2–28 mice. A strong nonspecific advential reaction was increased in the CKD-2–28 mice of unknown nature. α-Klotho was strongly expressed in the aortic media of wild-type (WT) and sham-operated mice, but was severely reduced in the stage 2 CKD mice. Immunohistochemistry (IHC) for α-Klotho was uniform in five WT, sham, and CKD-2 mice. The use of a nonspecific immunoglobulin G (IgG) in place of the primary antibody produced nonspecific positivity by both the secondary antibodies for FGF23 as well as klotho. (**d**) Plasma c-klotho levels were increased several fold in the CKD-2 mice at 15 and 22 weeks.

Runx2 expression has become its hallmark biomarker.[42] Runx2 expression in the aortic media was increased in our CKD-2 mice as compared with the *ldlr* − / − high fat–fed, sham-operated controls. A new key pathogenetic mechanism of vascular calcification in CKD, reduction of medial α-klotho activity,[30,32] was demonstrated in the aortic media of the CKD-2 mice by western blot analyses, histology, and message levels. As klotho antagonizes endothelial injury,[43] these findings may suggest an underappreciated role of endothelial injury in our model and in CKD-stimulated

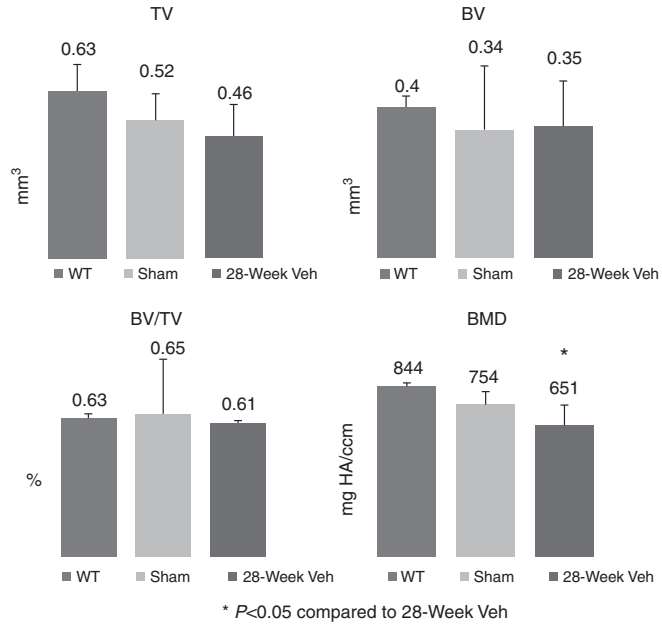

Figure 6 | Cortical bone micro-computed tomography (microCT) in *low-density lipoprotein–deficient* (*ldlr* − / −) high fat–fed mice with chronic kidney disease (CKD) stage 2. There was a decline in total volume (TV) and in bone mineral density (BMD) in the CKD-2 mice; $n = 10$. BV, bone volume; Veh, vehicle; WT, wild type.

vascular calcification. Our results agree with early reduction of renal klotho shown by Hu *et al.*,[30] but their studies suggested that the function of vascular klotho was inhibition of the phosphate stimulation of vascular calcification, whereas our studies show that CKD stimulation of vascular calcification was before the disruption of phosphate homeostasis. The FGFR/α-klotho ligand, FGF23, was found to be surprisingly induced in the aortic media of the sham-operated *ldlr* − / − high fat–fed mice and decreased by CKD-2. CKD-2 also stimulated an FGF23 advential immunolocalization reaction that may have represented circulating FGF23 bound to receptors. The localization of FGF23 suggests that osteocytic differentiation, which stems from osteoblasts, may have been the mechanism of FGF23 expression, in agreement with the findings of Zhu *et al.*,[44] and that the increase in FGF23 expression may represent a defense against vascular calcification, as first suggested by Voigt *et al.*[31] Scialla *et al.*[45] found in the CRIC cohort that FGF23 levels were not associated with vascular calcification. Our studies are one of the first to report CKD-stimulated vascular FGF23 expression, specifically in the aorta. This establishes a potential paracrine role of FGF23 interacting with medial klotho/FGFR. The reduction of klotho expression in the aortic media in CKD stage 2 mice indicates a potential resistance to FGF23 actions in the vasculature, and raises the issue of the role of FGF23 in vascular calcification that could not be addressed in these studies. Lim *et al.*[32] recently reported that the reduction of vascular klotho contributes to vascular calcification and causes resistance to the actions of FGF23 that, although not characterized, were thought to be resistive to vascular calcification. Lim *et al.*[32] and Donate-Correa *et al.*[43] did not find evidence for vascular FGF23 expression, although others[31] did, in agreement with our results.

The picture of the CKD–MBD syndrome in early CKD shows multiple evidences of skeletal effects produced by kidney disease. Our results demonstrated inhibition of bone formation rates, a decrease in cortical bone mineral density, a decreased bone area, and increased osteocytic secretion in the CKD-2 mice. Sabbagh *et al.*[21] showed that reduction of nuclear β-catenin, a manifestation of decreased Wnt signaling, and decreased skeletal anabolism was the earliest detected skeletal abnormality in CKD, and Pereira *et al.*[19] showed that FGF23 levels derived from skeletal osteocytes were increased in stage 2 CKD. Clinical and translational studies in models other than that used here and by Fang *et al.*[20] fail to demonstrate the decrease in bone formation reported in our studies. Rather, they show gradual development of high-turnover osteodystrophy compatible with the effects of increased PTH.[6,21,46,47] The likely explanation for this is the restriction to osteoblastogenesis imposed by the high peroxisome proliferator–activated receptor-γ activity in our model.[48] The resultant resistance to adaptive stimulation of bone formation by PTH permits the effects of kidney injury to inhibit bone formation to be observed in our model despite the development of secondary hyperparathyroidism. Despite the absence of a decrease in bone formation in early CKD, studies by Sabbagh *et al.*[21] indicate that decreased skeletal Wnt signaling is the earliest manifestation of the CKD–MBD detected in the *jck* mouse, a model of polycystic kidney disease, despite their observation of a gradual onset of high-turnover renal osteodystrophy by stage 3 CKD. Thus, early CKD affects the skeleton, and this may represent the onset of the CKD–MBD. The effects of early CKD on the skeleton shown here produced a low-turnover osteodystrophy and a decrease in cortical bone mineral density. Because of the still poorly characterized 'bone-vascular axis,' our findings of this osteodystrophy have to be considered in the pathogenetic mechanisms of the vascular calcification that we demonstrate to be stimulated by early CKD.

Two markers of osteocytic secretory activity, FGF23 and sclerostin, were increased in the CKD-2 mice. Activation of osteocytic FGF23 secretion is thought to be phosphate dependent, but the location of the sensing mechanism was unknown and FGF23 regulation in normophosphatemia unexplained. The recent discovery of the hormonal role of the cleavage product produced by proteolytic cleavage of the extracellular domain of α-klotho clarifies that the distal tubule sensing increased phosphate delivery, and producing c-klotho may be a mechanism of stimulating FGF23 secretion in early CKD in the presence of normal serum phosphate.[39] We found that c-klotho levels were elevated in the CKD-2 mice compatible with the marked increase in FGF23 and the normal serum phosphate. Several studies, such as those of Seiler *et al.*,[49] suggest that c-klotho levels decline during CKD in concert with the loss of renal α-klotho expression. However, our model of CKD-2 results from hypertrophy of a remnant kidney following AKI. The loss of α-klotho occur-

ring during the kidney injury phase is recovered during hypertrophy, as shown in the immunohistochemistry of the CKD-2 kidneys (Supplementary Figure S4 online). Thus, there is sufficient α-klotho substrate for the production of c-klotho by tubular phosphate—stimulated ADAM-17 and -10. Thus, our results are one of the first to suggest that, in early CKD before hyperphosphatemia, the mechanism of increased FGF23 secretion may be mediated by c-klotho. The complex situation of the kinetics of klotho expression in the face of decreased transcription and increased proteolytic cutting by ADAM-17 and -10 require careful study. In addition, the effects of tubular phosphate on ADAM-17 and -10 activity require further study.

The novel findings reported here are staging of CKD by BUN and inulin clearances in mice; the stimulation of vascular calcification by CKD equivalent to human stage 2 CKD (CKD-2 mice) before hyperphosphatemia; reduction of vascular α-klotho in early CKD; increased c-klotho as a means to increased FGF23 secretion in normophosphatemic CKD; and increased sclerostin levels and inhibition of bone formation in early CKD. In conclusion, early CKD induced in a model of atherosclerosis, stimulated vascular calcification and mesenchymal osteoblastic transition in the vasculature, inhibited bone formation, elevated FGF23 and sclerostin levels, and decreased aortic medial klotho expression. Ca and Pi levels were normal in early CKD, and PTH levels that were increased by AKI tended to normalize in CKD stage 2, whereas FGF23 levels continued to increase.

MATERIALS AND METHODS

Animals and diets

The *ldlr*$-/-$ mice of both genders in a C57Bl6 background were purchased from the Jackson Laboratory (Bar Harbor, ME) and were bred in a pathogen-free environment. Animals were weaned at 3 weeks to a chow diet (1:1 mixture of PicoLab (LabDiet, St Louis, MO) rodent chow 20 and mouse chow 20; 6.75% calories as fat). At 10 weeks, animals were continued on this chow diet or initiated on a high-cholesterol (0.15%) diet containing 42% calories as fat (Harlan Teklad, Madison, WI, product no. TD.88137), 0.6% Pi, 0.6% Ca, and vitamin D content 2.2 IU/g, a diet that has been shown to generate atherosclerosis with vascular calcification in this genetic background. At 12 weeks, CKD was induced as described in Supplementary Methods online. Animals had access to water *ad libitum*, and were maintained according to local and national animal care guidelines. The Washington University Animal Care Committee approved the study protocol.

DISCLOSURE

KAH reports having received research funding from Fresenius, Shire, Celgene, and Amgen. HM reports having received funding from Shire and Fresenius. KAH and HM have been consultants for Shire and Fresenius. All the other authors declared no competing interests.

ACKNOWLEDGMENTS

This research was supported by NIH grants DK070790 (to KAH) and DK089137 (to KAH), by an investigator-stimulated trial grant from Fresenius, and by the Kentucky Nephrology Research Trust.

SUPPLEMENTARY MATERIAL

Figure S1. Trabecular bone microCT in ldlr$-/-$ high fat fed mice with CKD stage 2.
Figure S2. Aortic calcium levels in ldlr$-/-$ high fat fed mice with CKD-3.
Figure S3. Plasma sclerostin levels in ldlr$-/-$ high fat fed CKD-2–28 and CKD-3–28 mice.
Figure S4. Immunolocalization of αklotho in the kidneys of the various groups of mice.
Supplementary material is linked to the online version of the paper at http://www.nature.com/ki

REFERENCES

1. Moe S, Drueke T, Cunningham J *et al.* Definition, evaluation, and classification of renal osteodystrophy: a position statement from Kidney Disease: Improving Global Outcomes (KDIGO). *Kidney Int* 2006; **69**: 1945–1953.
2. Go AS, Chertow GM, Fan D *et al.* Chronic kidney disease and the risks of death, cardiovascular events, and hospitalization. *New Engl J Med* 2004; **351**: 1296–1305.
3. Block GA, Hulbert-Shearon TE, Levin NW *et al.* Association of serum phosphorus and calcium X phosphate product with mortality risk in chronic hemodialysis patients: a national study. *Am J Kidney Dis* 1998; **31**: 607–617.
4. Kestenbaum B, Sampson JN, Rudser KD *et al.* Serum phosphate levels and mortality risk among people with chronic kidney disease. *J Am Soc Nephrol* 2005; **16**: 520–528.
5. Keith DS, Nichols GA, Gullion CM *et al.* Longitudinal follow-up and outcomes among a population with chronic kidney disease in a large managed care organization. *Arch Intern Med* 2004; **164**: 659–663.
6. Moe SM, Radcliffe JS, White KE *et al.* The pathophysiology of early-stage chronic kidney disease–mineral bone disorder (CKD-MBD) and response to phosphate binders in the rat. *J Bone Miner Res* 2011; **26**: 2672–2681.
7. Blacher J, Guerin AP, Pannier B *et al.* Arterial calcifications, arterial stiffness, and cardiovascular risk in end-stage renal disease. *Hypertension* 2001; **38**: 938–942.
8. London GM, Guerin AP, Marchais SJ *et al.* Arterial media calcification in end-stage renal diseases: impact on all-cause and cardiovascular mortality. *Nephrol Dial Transplant* 2003; **18**: 1731–1740.
9. Hruska K, Mathew S, Lund R *et al.* Cardiovascular risk factors in chronic kidney disease: does phosphate qualify? *Kidney Int* 2011; **79**(Suppl 121): S9–S13.
10. Gutierrez OM, Mannstadt M, Isakova T *et al.* Fibroblast growth factor 23 and mortality among patients undergoing hemodialysis. *New Engl J Med* 2008; **359**: 584–592.
11. Arnlov J, Carlsson AC, Sundstrom J *et al.* Higher fibroblast growth factor-23 increases the risk of all-cause and cardiovascular mortality in the community. *Kidney Int* 2013; **83**: 160–166.
12. Rennenberg RJMW Kessels AGH, Schurgers LJ *et al.* Vascular calcifications as a marker of increased cardiovascular risk: a meta-analysis. *Vasc Health Risk Manag* 2009; **5**: 185–197.
13. Moe SM, Chen NX. Pathophysiology of vascular calcification in chronic kidney disease. *Circ Res* 2004; **95**: 560–567.
14. Mathew S, Lund R, Strebeck F *et al.* Reversal of the adynamic bone disorder and decreased vascular calcification in chronic kidney disease by sevelamer carbonate therapy. *J Am Soc Nephrol* 2007; **18**: 122–130.
15. El-Abbadi MM, Pai AS, Leaf EM *et al.* Phosphate feeding induces arterial medial calcification in uremic mice: role of serum phosphorus, fibroblast growth factor-23, and osteopontin. *Kidney Int* 2009; **75**: 1297–1307.
16. Chen NX, O'Neill KD, Duan D *et al.* Phosphorus and uremic serum up-regulate osteopontin expression in vascular smooth muscle cells. *Kidney Int* 2002; **62**: 1724–1731.
17. Shanahan CM, Crouthamel MH, Kapustin A *et al.* Arterial calcification in chronic kidney disease: key roles for calcium and phosphate. *Circ Res* 2011; **109**: 697–711.
18. Hill KM, Martin BR, Wastney ME *et al.* Oral calcium carbonate affects calcium but not phosphorus balance in stage 3-4 chronic kidney disease. *Kidney Int* 2012; **83**: 959–966.
19. Pereira RC, Juppner H, Azucena-Serrano CE *et al.* Patterns of FGF-23, DMP1 and MEPE expression in patients with chronic kidney disease. *Bone* 2009; **45**: 1161–1168.
20. Fang Y, Zhang Y, Mathew S *et al.* Early chronic kidney disease (CKD) stimulates vascular calcification (VC) and decreased bone formation rates prior to positive phosphate balance. *J Am Soc Nephrol* 2009; **20**: 36A.

21. Sabbagh Y, Graciolli FG, O'Brien S *et al.* Repression of osteocyte Wnt/β-catenin signaling is an early event in the progression of renal osteodystrophy. *J Bone Miner Res* 2012; **27**: 1757–1772.
22. Oliveira RB, Cancela ALE, Graciolli FG *et al.* Early control of PTH and FGF23 in normophosphatemic CKD patients: a new target in CKD-MBD therapy? *Clin J Am Soc Nephrol* 2010; **5**: 286–291.
23. Isakova T, Wahl P, Vargas GS *et al.* Fibroblast growth factor 23 is elevated before parathyroid hormone and phosphate in chronic kidney disease. *Kidney Int* 2011; **79**: 1370–1378.
24. Babij P, Zhao W, Small C *et al.* High bone mass in mice expressing a mutant LRP5 gene. *J Bone Miner Res* 2003; **18**: 960–974.
25. Little RD, Carulli JP, DelMastro RG *et al.* A mutation in the LDL receptor-related protein 5 gene results in the autosomal dominant high-bone-mass trait. *Am J Hum Genet* 2002; **70**: 11–19.
26. Lund RJ, Davies MR, Brown AJ *et al.* Successful treatment of an adynamic bone disorder with bone morphogenetic protein-7 in a renal ablation model. *J Am Soc Nephrol* 2004; **15**: 359–369.
27. Mahmoodi BK, Matsushita K, Woodward M *et al.* Associations of kidney disease measures with mortality and end-stage renal disease in individuals with and without hypertension: a meta-analysis. *Lancet* 2012; **380**: 1649–1661.
28. Fox CS, Matsushita K, Woodward M *et al.* Associations of kidney disease measures with mortality and end-stage renal disease in individuals with and without diabetes: a meta-analysis. *Lancet* 2012; **380**: 1662–1673.
29. Davies MR, Lund RJ, Hruska KA. BMP-7 is an efficacious treatment of vascular calcification in a murine model of atherosclerosis and chronic renal failure. *J Am Soc Nephrol* 2003; **14**: 1559–1567.
30. Hu MC, Shi M, Zhang J *et al.* Klotho deficiency causes vascular calcification in chronic kidney disease. *J Am Soc Nephrol* 2011; **22**: 124–136.
31. Voigt M, Fischer D-C, Rimpau M *et al.* Fibroblast growth factor (FGF)-23 and fetuin-A in calcified carotid atheroma. *Histopathology* 2010; **56**: 775–788.
32. Lim K, Lu T-S, Molostvov G *et al.* Vascular klotho deficiency potentiates the development of human artery calcification and mediates resistance to fibroblast growth factor 23. *Circulation* 2012; **125**: 2243–2255.
33. Davies MR, Lund RJ, Mathew S *et al.* Low turnover osteodystrophy and vascular calcification are amenable to skeletal anabolism in an animal model of chronic kidney disease and the metabolic syndrome. *J Am Soc Nephrol* 2005; **16**: 917–928.
34. Ben-Dov IZ, Galitzer H, Lavi-Moshayoff V *et al.* The parathyroid is a target organ for FGF23 in rats. *J Clin Invest* 2007; **117**: 4003–4008.
35. London GM. Cardiovascular calcifications in uremic patients: clinical impact on cardiovascular function. *J Am Soc Nephrol* 2003; **14**: S305–S309.
36. Mathew S, Tustison KS, Sugatani T *et al.* The mechanism of phosphorus as a cardiovascular risk factor in chronic kidney disease. *J Am Soc Nephrol* 2008; **19**: 1092–1105.
37. Speer MY, Yang HY, Brabb T *et al.* Smooth muscle cells give rise to osteochondrogenic precursors and chondrocytes in calcifying arteries. *Circ Res* 2009; **104**: 733–741.
38. Shanahan CM, Cary NRB, Salisbury JR *et al.* Medial localization of mineralization-regulating proteins in association with Monckeberg's sclerosis: evidence for smooth muscle cell-mediated vascular calcification. *Circulation* 1999; **100**: 2168–2176.
39. Smith RC, O'Bryan LM, Farrow EG *et al.* Circulating αKlotho influences phosphate handling by controlling FGF23 production. *J Clin Invest* 2012; **122**: 4710–4715.
40. Cejka D, Herberth J, Branscum AJ *et al.* Sclerostin and Dickkopf-1 in renal osteodystrophy. *Clin J Am Soc Nephrol* 2011; **6**: 877–882.
41. Shanahan CM, Proudfoot D, Tyson KL *et al.* Expression of mineralisation-regulating proteins in association with human vascular calcification *Z Kardiol* 2000; **89**: S063–S068.
42. Moe SM, O'Neill KD, Duan D *et al.* Medial artery calcification in ESRD patients is associated with deposition of bone matrix proteins. *Kidney Int* 2002; **61**: 638–647.
43. Donate-Correa J, Mora-Fernández C, Martínez-Sanz R *et al.* Expression of FGF23/KLOTHO system in human vascular tissue. *Int J Cardiol* 2011; **165**: 179–183.
44. Zhu D, Mackenzie NCW, Millán JL *et al.* The appearance and modulation of osteocyte marker expression during calcification of vascular smooth muscle cells. *PLoS One* 2011; **6**: e19595.
45. Scialla JJ, Lau WL, Reilly MP *et al.* Fibroblast growth factor 23 is not associated with and does not induce arterial calcification. *Kidney Int* 2013; **83**: 1159–1168.
46. Slatopolsky E, Caglar S, Pennell JP. On the pathogenesis of hyperparathyroidism in chronic experimental insufficiency in the dog. *J Clin Invest* 1971; **50**: 492–499.
47. Stubbs JR, He N, Idiculla A *et al.* Longitudinal evaluation of FGF23 changes and mineral metabolism abnormalities in a mouse model of chronic kidney disease. *J Bone Miner Res* 2012; **27**: 38–46.
48. Lecka-Czernik B, Gubrij I, Moerman EJ *et al.* Inhibition of Osf2/Cbfa1 expression and terminal osteoblast differentiation by PPARgamma2. *J Cell Biochem* 1999; **74**: 347–371.
49. Seiler S, Wen M, Roth HJ *et al.* Plasma Klotho is not related to kidney function and does not predict adverse outcome in patients with chronic kidney disease. *Kidney Int* 2013; **83**: 121–128.